

¹ Critical transitions and the fragmenting of global forests

² Leonardo A. Saravia^{1 3}, Santiago R. Doyle¹, Benjamin Bond-Lamberty²

³ 1. Instituto de Ciencias, Universidad Nacional de General Sarmiento, J.M. Gutierrez 1159 (1613), Los
⁴ Polvorines, Buenos Aires, Argentina.

⁵ 2. Pacific Northwest National Laboratory, Joint Global Change Research Institute at the University of
⁶ Maryland–College Park, 5825 University Research Court #3500, College Park, MD 20740, USA

⁷ 3. Corresponding author e-mail: lsaravia@ungs.edu.ar

⁸ **keywords:** Forest fragmentation, early warning signals, percolation, power-laws, MODIS, critical transitions

⁹ **Running title:** Critical fragmentation in global forest

¹⁰ **number of words in abstract:** 298

¹¹ **number of words in the article:** 5568

¹² **number of references:** 84

¹³ Abstract

¹⁴ 1. Forests provide critical habitat for many species, essential ecosystem services, and are coupled to
¹⁵ atmospheric dynamics through exchanges of energy, water and gases. One of the most important
¹⁶ changes produced in the biosphere is the replacement of forest areas with human dominated landscapes.
¹⁷ This usually leads to fragmentation, altering the sizes of patches, the structure and function of the
¹⁸ forest. Here we studied the distribution and dynamics of forest patch sizes at a global level, examining
¹⁹ signals of a critical transition from an unfragmented to a fragmented state.

²⁰ 2. We used MODIS vegetation continuous field to estimate the forest patches at a global level and defined
²¹ wide regions of connected forest across continents and big islands. We search for critical phase transitions,
²² where the system state of the forest changes suddenly at a critical point; this implies an abrupt
²³ change in connectivity that causes a increased fragmentation level. We studied the distribution of for-
²⁴ est patch sizes and the dynamics of the largest patch over the last fourteen years. The conditions that
²⁵ indicate that a region is near a critical fragmentation threshold are related to patch size distribution
²⁶ and temporal fluctuations of the largest patch.

²⁷ 3. We found that most regions, except the Eurasian mainland, followed a power-law distribution. Only
²⁸ the tropical forest of Africa and South America met the criteria to be near a critical fragmentation

29 threshold.

- 30 4. This implies that human pressures and climate forcings might trigger undesired effects of fragmentation,
31 such as species loss and degradation of ecosystems services, in these regions. The simple criteria
32 proposed here could be used as early warning to estimate the distance to a fragmentation threshold in
33 forest around the globe and could be used as a predictor of a planetary tipping point.

³⁴ Introduction

³⁵ Forests are one of the most important ecosystems on earth, providing habitat for a large proportion of species
³⁶ and contributing extensively to global biodiversity (Crowther *et al.* 2015). In the previous century human
³⁷ activities have influenced global bio-geochemical cycles (Bonan 2008; Canfield, Glazer & Falkowski 2010),
³⁸ with one of the most dramatic changes being the replacement of 40% of Earth's formerly biodiverse land
³⁹ areas with landscapes that contain only a few species of crop plants, domestic animals and humans (Foley
⁴⁰ *et al.* 2011). These local changes have accumulated over time and now constitute a global forcing (Barnosky
⁴¹ *et al.* 2012).

⁴² Another global scale forcing that is tied to habitat destruction is fragmentation, which is defined as the
⁴³ division of a continuous habitat into separated portions that are smaller and more isolated. Fragmentation
⁴⁴ produces multiple interwoven effects: reductions of biodiversity between 13% and 75%, decreasing forest
⁴⁵ biomass, and changes in nutrient cycling (Haddad *et al.* 2015). The effects of fragmentation are not only
⁴⁶ important from an ecological point of view but also that of human activities, as ecosystem services are deeply
⁴⁷ influenced by the level of landscape fragmentation (Mitchell *et al.* 2015).

⁴⁸ Ecosystems have complex interactions between species and present feedbacks at different levels of organiza-
⁴⁹ tion (Gilman *et al.* 2010), and external forcings can produce abrupt changes from one state to another,
⁵⁰ called critical transitions (Scheffer *et al.* 2009). These abrupt state shifts cannot be linearly forecasted from
⁵¹ past changes, and are thus difficult to predict and manage (Scheffer *et al.* 2009). Critical transitions have
⁵² been detected mostly at local scales (Drake & Griffen 2010; Carpenter *et al.* 2011), but the accumulation of
⁵³ changes in local communities that overlap geographically can propagate and theoretically cause an abrupt
⁵⁴ change of the entire system at larger scales (Barnosky *et al.* 2012). Coupled with the existence of global
⁵⁵ scale forcings, this implies the possibility that a critical transition could occur at a global scale (Rockstrom
⁵⁶ *et al.* 2009; Folke *et al.* 2011).

⁵⁷ Complex systems can experience two general classes of critical transitions (Solé 2011). In so-called first
⁵⁸ order transitions, a catastrophic regime shift that is mostly irreversible occurs because of the existence of
⁵⁹ alternative stable states (Scheffer *et al.* 2001). This class of transitions is suspected to be present in a variety
⁶⁰ of ecosystems such as lakes, woodlands, coral reefs (Scheffer *et al.* 2001), semi-arid grasslands (Bestelmeyer
⁶¹ *et al.* 2011), and fish populations (Vasilakopoulos & Marshall 2015). They can be the result of positive
⁶² feedback mechanisms (Martín *et al.* 2015); for example, fires in some forest ecosystems were more likely to
⁶³ occur in previously burned areas than in unburned places (Kitzberger *et al.* 2012).

⁶⁴ The other class of critical transitions are continuous or second order transitions (Solé & Bascompte 2006).

65 In these cases, there is a narrow region where the system suddenly changes from one domain to another,
66 with the change being continuous and in theory reversible. This kind of transitions were suggested to be
67 present in tropical forest (Pueyo *et al.* 2010), semi-arid mountain ecosystems (McKenzie & Kennedy 2012),
68 tundra shrublands (Naito & Cairns 2015). The transition happens at critical point where we can observe a
69 distinctive spatial pattern: scale invariant fractal structures characterized by power law patch distributions
70 (Stauffer & Aharony 1994).

71 There are several processes that can convert a catastrophic transition to a second order transitions (Martín
72 *et al.* 2015). These include stochasticity, such as demographic fluctuations, spatial heterogeneities, and/or
73 dispersal limitation. All these components are present in forest around the globe (Seidler & Plotkin 2006;
74 Filotas *et al.* 2014; Fung *et al.* 2016), thus continuous transitions might be more probable than catastrophic
75 transitions. Moreover there is some evidence of recovery in some systems that supposedly suffered an
76 irreversible transition produced by overgrazing (Zhang *et al.* 2005) and desertification (Allington & Valone
77 2010).

78 The spatial phenomena observed in continuous critical transitions deal with connectivity, a fundamental
79 property of general systems and ecosystems from forests (Ochoa-Quintero *et al.* 2015) to marine ecosystems
80 (Leibold & Norberg 2004) and the whole biosphere (Lenton & Williams 2013). When a system goes from a
81 fragmented to a connected state we say that it percolates (Solé 2011). Percolation implies that there is a
82 path of connections that involves the whole system. Thus we can characterize two domains or phases: one
83 dominated by short-range interactions where information cannot spread, and another in which long range
84 interactions are possible and information can spread over the whole area. (The term “information” is used
85 in a broad sense and can represent species dispersal or movement.)

86 Thus, there is a critical “percolation threshold” between the two phases, and the system could be driven
87 close to or beyond this point by an external force; climate change and deforestation are the main forces
88 that could be the drivers of such a phase change in contemporary forests (Bonan 2008; Haddad *et al.* 2015).
89 There are several applications of this concept in ecology: species’ dispersal strategies are influenced by
90 percolation thresholds in three-dimensional forest structure (Solé, Bartumeus & Gamarra 2005), and it has
91 been shown that species distributions also have percolation thresholds (He & Hubbell 2003). This implies
92 that pushing the system below the percolation threshold could produce a biodiversity collapse (Bascompte
93 & Solé 1996; Solé, Alonso & Saldaña 2004; Pardini *et al.* 2010); conversely, being in a connected state (above
94 the threshold) could accelerate the invasion of forest into prairie (Loehle, Li & Sundell 1996; Naito & Cairns
95 2015).

96 One of the main challenges with systems that can experience critical transitions—of any kind—is that the

97 value of the critical threshold is not known in advance. In addition, because near the critical point a small
98 change can precipitate a state shift of the system, they are difficult to predict. Several methods have been
99 developed to detect if a system is close to the critical point, e.g. a deceleration in recovery from perturbations,
100 or an increase in variance in the spatial or temporal pattern (Hastings & Wysham 2010; Carpenter *et al.*
101 2011; Boettiger & Hastings 2012; Dai *et al.* 2012).

102 In this study, our objective is to look for evidence that forests around the globe are near continuous critical
103 point that represent a fragmentation threshold. We use the framework of percolation to first evaluate if
104 forest patch distribution at a continental scale is described by a power law distribution and then examined
105 the fluctuations of the largest patch. The advantage of using data at a continental scale is that for very large
106 systems the transitions are very sharp (Solé 2011) and thus much easier to detect than at smaller scales,
107 where noise can mask the signals of the transition.

108 Methods

109 Study areas definition

110 We analyzed mainland forests at a continental scale, covering the whole globe, by delimiting land areas with
111 a near-contiguous forest cover, separated with each other by large non-forested areas. Using this criterion,
112 we delimited the following forest regions. In America, three regions were defined: South America temperate
113 forest (SAT), subtropical and tropical forest up to Mexico (SAST), and USA and Canada forest (NA). Europe
114 and North Asia were treated as one region (EUAS). The rest of the delimited regions were South-east Asia
115 (SEAS), Africa (AF), and Australia (OC). We also included in the analysis islands larger than 10^5 km². The
116 mainland region has the number 1 e.g. OC1, and the nearby islands have consecutive numeration (Appendix
117 S4, figure S1-S6).

118 Forest patch distribution

119 We studied forest patch distribution in each defined area from 2000 to 2014 using the MODerate-resolution
120 Imaging Spectroradiometer (MODIS) Vegetation Continuous Fields (VCF) Tree Cover dataset version 051
121 (DiMiceli *et al.* 2015). This dataset is produced at a global level with a 231-m resolution, from 2000 onwards
122 on an annual basis. There are several definition of forest based on percent tree cover (Sexton *et al.* 2015),
123 we choose a 30% threshold to convert the percentage tree cover to a binary image of forest and non-forest
124 pixels. This was the definition used by the United Nations' International Geosphere-Biosphere Programme
125 (Belward 1996), and studies of global fragmentation (Haddad *et al.* 2015). This definition avoids the errors

126 produced by low discrimination of MODIS VCF between forest and dense herbaceous vegetation at low forest
127 cover (Sexton *et al.* 2015). Patches of contiguous forest were determined in the binary image by grouping
128 connected forest pixels using a neighborhood of 8 forest units (Moore neighborhood).

129 **Percolation theory**

130 A more in-depth introduction to percolation theory can be found elsewhere (Stauffer & Aharony 1994) and
131 a review from an ecological point of view is available (Oborny, Szabó & Meszéna 2007). Here, to explain
132 the basic elements of percolation theory we formulate a simple model: we represent our area of interest by a
133 square lattice and each site of the lattice can be occupied—e.g. by forest—with a probability p . The lattice
134 will be more occupied when p is greater, but the sites are randomly distributed. We are interested in the
135 connection between sites, so we define a neighborhood as the eight adjacent sites surrounding any particular
136 site. The sites that are neighbors of other occupied sites define a patch. When there is a patch that connects
137 the lattice from opposite sides, it is said that the system percolates. When p is increased from low values, a
138 percolating patch suddenly appears at some value of p called the critical point p_c .

139 Thus percolation is characterized by two well defined phases: the unconnected phase when $p < p_c$ (called
140 subcritical in physics), in which species cannot travel far inside the forest, as it is fragmented; in a general
141 sense, information cannot spread. The second is the connected phase when $p > p_c$ (supercritical), species
142 can move inside a forest patch from side to side of the area (lattice), i.e. information can spread over the
143 whole area. Near the critical point several scaling laws arise: the structure of the patch that spans the area
144 is fractal, the size distribution of the patches is power-law, and other quantities also follow power-law scaling
145 (Stauffer & Aharony 1994).

146 The value of the critical point p_c depends on the geometry of the lattice and on the definition of the
147 neighborhood, but other power-law exponents only depend on the lattice dimension. Close to the critical
148 point, the distribution of patch sizes is:

149 (1) $n_s(p_c) \propto s^{-\alpha}$

150 where $n_s(p)$ is the number of patches of size s . The exponent α does not depend on the details of the
151 model and it is called universal (Stauffer & Aharony 1994). These scaling laws can be applied for landscape
152 structures that are approximately random, or at least only correlated over short distances (Gastner *et al.*
153 2009). In physics this is called “isotropic percolation universality class”, and corresponds to an exponent
154 $\alpha = 2.05495$. If we observe that the patch size distribution has another exponent it will not belong to this
155 universality class and some other mechanism should be invoked to explain it. Percolation thresholds can also

156 be generated by models that have some kind of memory (Hinrichsen 2000; Ódor 2004): for example, a patch
157 that has been exploited for many years will recover differently than a recently deforested forest patch. In
158 this case, the system could belong to a different universality class, or in some cases there is no universality,
159 in which case the value of α will depend on the parameters and details of the model (Corrado, Cherubini &
160 Pennetta 2014).

161 To illustrate these concepts, we conducted simulations with a simple forest model with only two states:
162 forest and non-forest. This type of model is called a “contact process” and was introduced for epidemics
163 (Harris 1974), but has many applications in ecology (Solé & Bascompte 2006; Gastner *et al.* 2009). A site
164 with forest can become extinct with probability e , and produce another forest site in a neighborhood with
165 probability c . We use a neighborhood defined by an isotropic power law probability distribution. We defined
166 a single control parameter as $\lambda = c/e$ and ran simulations for the subcritical fragmentation state $\lambda < \lambda_c$,
167 with $\lambda = 2$, near the critical point for $\lambda = 2.5$, and for the supercritical state with $\lambda = 5$ (see Appendix S2,
168 gif animations).

169 Patch size distributions

170 We fitted the empirical distribution of forest patch areas, based on the MODIS-derived data described above,
171 to four distributions using maximum likelihood estimation (Goldstein, Morris & Yen 2004; Clauset, Shalizi
172 & Newman 2009). The distributions were: power-law, power-law with exponential cut-off, log-normal, and
173 exponential. We assumed that the patch size distribution is a continuous variable that was discretized by
174 remote sensing data acquisition procedure.

175 We set a minimal patch size (X_{min}) at nine pixels to fit the patch size distributions to avoid artifacts at patch
176 edges due to discretization (Weerman *et al.* 2012). Besides this hard X_{min} limit we set due to discretization,
177 the power-law distribution needs a lower bound for its scaling behavior. This lower bound is also estimated
178 from the data by maximizing the Kolmogorov-Smirnov (KS) statistic, computed by comparing the empirical
179 and fitted cumulative distribution functions (Clauset *et al.* 2009). We also calculated the uncertainty of the
180 parameters using a non-parametric bootstrap method (Efron & Tibshirani 1994), and computed corrected
181 Akaike Information Criteria (AIC_c) and Akaike weights for each model (Burnham & Anderson 2002). Akaike
182 weights (w_i) are the weight of evidence in favor of model i being the actual best model given that one of the
183 N models must be the best model for that set of N models.

184 Additionally, we computed the goodness of fit of the power-law model following the bootstrap approach
185 described by Clauset et. al (2009), where simulated data sets following the fitted model are generated, and a

186 p -value computed as the proportion of simulated data sets that has a KS statistic less extreme than empirical
187 data. The criterion to reject the power law model suggested by Clauset et. al (2009) was $p \leq 0.1$, but as we
188 have a very large n , meaning that negligible small deviations could produce a rejection (Klaus, Yu & Plenz
189 2011), we chose a $p \leq 0.05$ to reject the power law model.

190 To test for differences between the fitted power law exponent for each study area we used a generalized least
191 squares linear model (Zuur *et al.* 2009) with weights and a residual auto-correlation structure. Weights were
192 the bootstrapped 95% confidence intervals and we added an auto-regressive model of order 1 to the residuals
193 to account for temporal autocorrelation.

194 **Largest patch dynamics**

195 The largest patch is the one that connects the highest number of sites in the area. This has been used
196 extensively to indicate fragmentation (Gardner & Urban 2007; Ochoa-Quintero *et al.* 2015). The relation of
197 the size of the largest patch S_{max} to critical transitions has been extensively studied in relation to percolation
198 phenomena (Stauffer & Aharony 1994; Bazant 2000; Botet & Ploszajczak 2004), but seldom used in ecological
199 studies (for an exception see Gastner *et al.* (2009)). When the system is in a connected state ($p > p_c$) the
200 landscape is almost insensitive to the loss of a small fraction of forest, but close to the critical point a minor
201 loss can have important effects (Solé & Bascompte 2006; Oborny *et al.* 2007), because at this point the
202 largest patch will have a filamentary structure, i.e. extended forest areas will be connected by thin threads.
203 Small losses can thus produce large fluctuations.

204 One way to evaluate the fragmentation of the forest is to calculate the proportion of the largest patch against
205 the total area (Keitt, Urban & Milne 1997). The total area of the regions we are considering (Appendix S4,
206 figures S1-S6) may not be the same than the total area that the forest could potentially occupy, thus a more
207 accurate way to evaluate the weight of S_{max} is to use the total forest area, that can be easily calculated
208 summing all the forest pixels. We calculate the proportion of the largest patch for each year, dividing S_{max}
209 by the total forest area of the same year: $RS_{max} = S_{max} / \sum_i S_i$. This has the effect of reducing the S_{max}
210 fluctuations produced due to environmental or climatic changes influences in total forest area. When the
211 proportion RS_{max} is large (more than 60%) the largest patch contains most of the forest so there are fewer
212 small forest patches and the system is probably in a connected phase. Conversely, when it is low (less than
213 20%), the system is probably in a fragmented phase (Saravia & Momo 2017).

214 The RS_{max} is a useful qualitative index that does not tell us if the system is near or far from the critical
215 transition; this can be evaluated using the temporal fluctuations. We calculate the fluctuations around the

216 mean with the absolute values $\Delta S_{max} = S_{max}(t) - \langle S_{max} \rangle$, using the proportions of RS_{max} . To characterize
217 fluctuations we fitted three empirical distributions: power-law, log-normal, and exponential, using the same
218 methods described previously. We expect that large fluctuation near a critical point have heavy tails (log-
219 normal or power-law) and that fluctuations far from a critical point have exponential tails, corresponding
220 to Gaussian processes (Rooij *et al.* 2013). As the data set spans 15 years, we do not have enough power to
221 reliably detect which distribution is better (Clauset *et al.* 2009). To improve this we performed the goodness
222 of fit test described above for all the distributions. We generated animated maps showing the fluctuations
223 of the two largest patches to aid in the interpretations of the results.

224 A robust way to detect if the system is near a critical transition is to analyze the increase in variance of
225 the density (Benedetti-Cecchi *et al.* 2015). It has been demonstrated that the variance increase in density
226 appears when the system is very close to the transition (Corrado *et al.* 2014), thus practically it does
227 not constitute an early warning indicator. An alternative is to analyze the variance of the fluctuations of
228 the largest patch ΔS_{max} : the maximum is attained at the critical point but a significant increase occurs
229 well before the system reaches the critical point (Corrado *et al.* 2014). In addition, before the critical
230 fragmentation, the skewness of the distribution of ΔS_{max} should be negative, implying that fluctuations
231 below the average are more frequent. We characterized the increase in the variance using quantile regression:
232 if variance is increasing the slopes of upper or/and lower quartiles should be positive or negative.

233 All statistical analyses were performed using the GNU R version 3.3.0 (R Core Team 2015), using code
234 provided by Cosma R. Shalizi for fitting the power law with exponential cutoff model and the poweRlaw
235 package (Gillespie 2015) for fitting the other distributions. For the generalized least squares linear model we
236 used the R function gls from package nlme (Pinheiro *et al.* 2016); and we fitted quantile regressions using
237 the R package quantreg (Koenker 2016). Image processing was done in MATLAB r2015b (The Mathworks
238 Inc.). The complete source code for image processing and statistical analysis, and the patch size data files
239 are available at figshare <http://dx.doi.org/10.6084/m9.figshare.4263905>.

240 Results

241 The figure 1 shows an example of the distribution of the biggest 200 patches for years 2000 and 2014,
242 this distribution is highly variable. The visual inspection could be used to detect the increase or decrease
243 of fragmentation in different areas of interest. The biggest patch usually maintain its location (but see
244 animations Appendix S3), smaller patches can merge or break more easily so they enter or leave the list of
245 200, and this is why there is a color change across years.

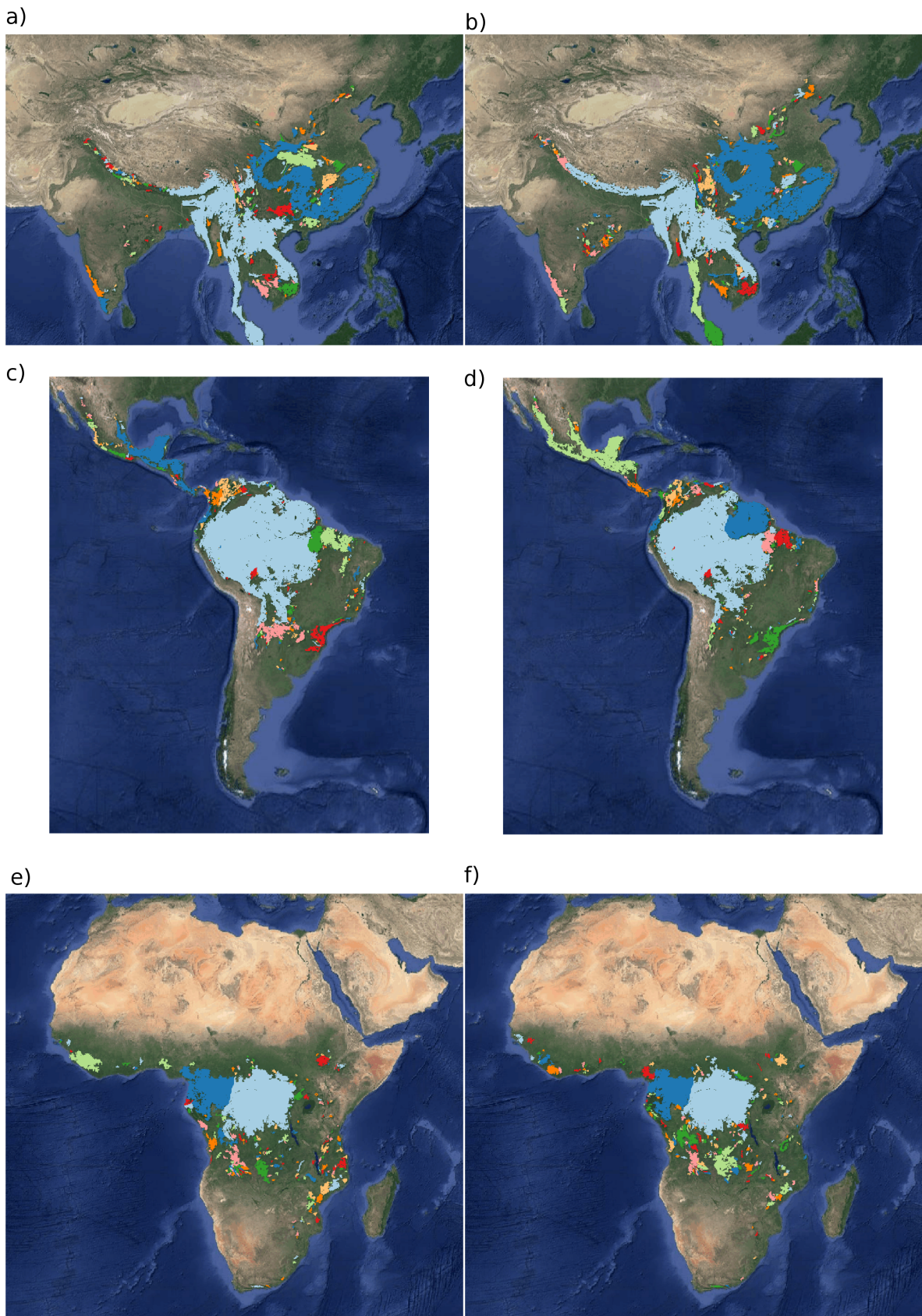


Figure 1: Forest patch distributions for continental regions for the years 2000 and 2014. The images are the 200 biggest patches, showed at a coarse pixel scale of 2.5 Km. The regions are: a) & b) southeast Asia; c) & d) South America subtropical and tropical and e) & f) Africa mainland, for the years 2000 and 2014 respectively.

246 The power law distribution was selected as the best model in 92% of the cases (Appendix S4, Figure S7).
247 In a small number of cases (1%) the power law with exponential cutoff was selected, but the value of the
248 parameter α was similar by ± 0.02 to the pure power law. Additionally the patch size where the exponential
249 tail begins is very large, thus we used the power law parameters for this cases (See Appendix S4, Figure S2,
250 region EUAS3). In finite-size systems the favored model should be the power law with exponential cutoff,
251 because the power-law tails are truncated to the size of the system (Stauffer & Aharony 1994). Here the
252 regions are so large that the cutoff is practically not observed.

253 There is only one region that did not follow a power law: Eurasia mainland, which showed a log-normal
254 distribution, representing 7% of the cases. The log-normal and power law are both heavy tailed distributions
255 and difficult to distinguish, but in this case Akaike weights have very high values for log-normal (near 1),
256 meaning that this is the only possible model. In addition, the goodness of fit tests clearly rejected the power
257 law model in all cases for this region (Appendix S4, table S1, region EUAS1). In general the goodness of fit
258 test rejected the power law model in fewer than 10% of cases. In large forest areas like Africa mainland (AF1)
259 or South America tropical-subtropical (SAST1), larger deviations are expected and the rejections rates are
260 higher so the proportion is 30% or less (Appendix S4, Table S1).

261 Taking into account the bootstrapped confidence intervals of each power law exponent (α) and the temporal
262 autocorrelation, there were no significant differences between α for the regions with the biggest (greater than
263 10^7 km^2) forest areas (Figure 2 and Appendix S4, Figure S8). There were also no differences between these
264 regions and smaller ones (Appendix S4, Tables S2 & S3), and all the slopes of α were not different from
265 0 (Appendix S4, Table S3). This implies a global average $\alpha = 1.908$, with a bootstrapped 95% confidence
266 interval between 1.898 and 1.920.

267 The proportion of the largest patch relative to total forest area RS_{max} for regions with more than 10^7 km^2
268 of forest is shown in figure 3. South America tropical and subtropical (SAST1) and North America (NA1)
269 have a higher RS_{max} of more than 60%, and other big regions 40% or less. For regions with less total
270 forest area (Appendix S4, figure S9 & Table 1), the United Kingdom (EUAS3) has a very low proportion
271 near 1%, while other regions such as New Guinea (OC2) and Malaysia/Kalimantan (OC3) have a very high
272 proportion. SEAS2 (Philippines) is a very interesting case because it seems to be under 30% until the year
273 2005, fluctuates in the range 30-60%, and then stays over 60% (Appendix S4, figure S9).

274 We analyzed the distributions of fluctuations of the largest patch relative to total forest area ΔRS_{max}
275 and the fluctuations of the largest patch ΔS_{max} . The model selection for ΔS_{max} resulted in power law
276 distributions for all regions (Appendix S4, table S6). For ΔRS_{max} instead some regions showed exponential
277 distributions: Eurasia mainland (EUAS1), New Guinea (OC2), Malaysia (OC3), New Zealand (OC6, OC8)

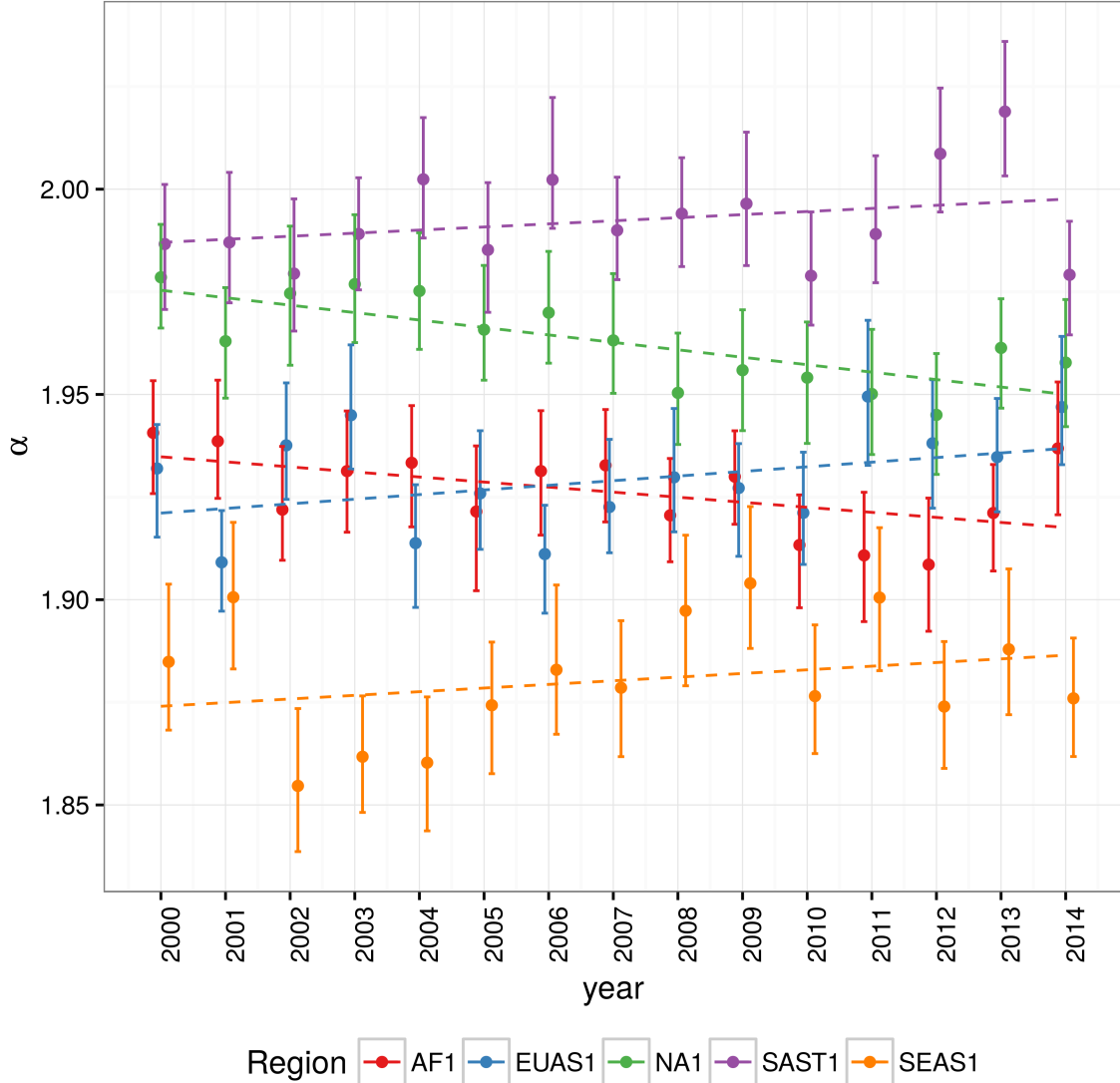


Figure 2: Power law exponents (α) of forest patch distributions for regions with total forest area $> 10^7 \text{ km}^2$. Dashed horizontal lines are the fitted generalized least squares linear model, with 95% confidence interval error bars estimated by bootstrap resampling. The regions are AF1: Africa mainland, EUAS1: Eurasia mainland, NA1: North America mainland, SAST1: South America subtropical and tropical, SEAS1: Southeast Asia mainland. For EUAS1 the best model is log-normal but the exponents are included here for comparison.

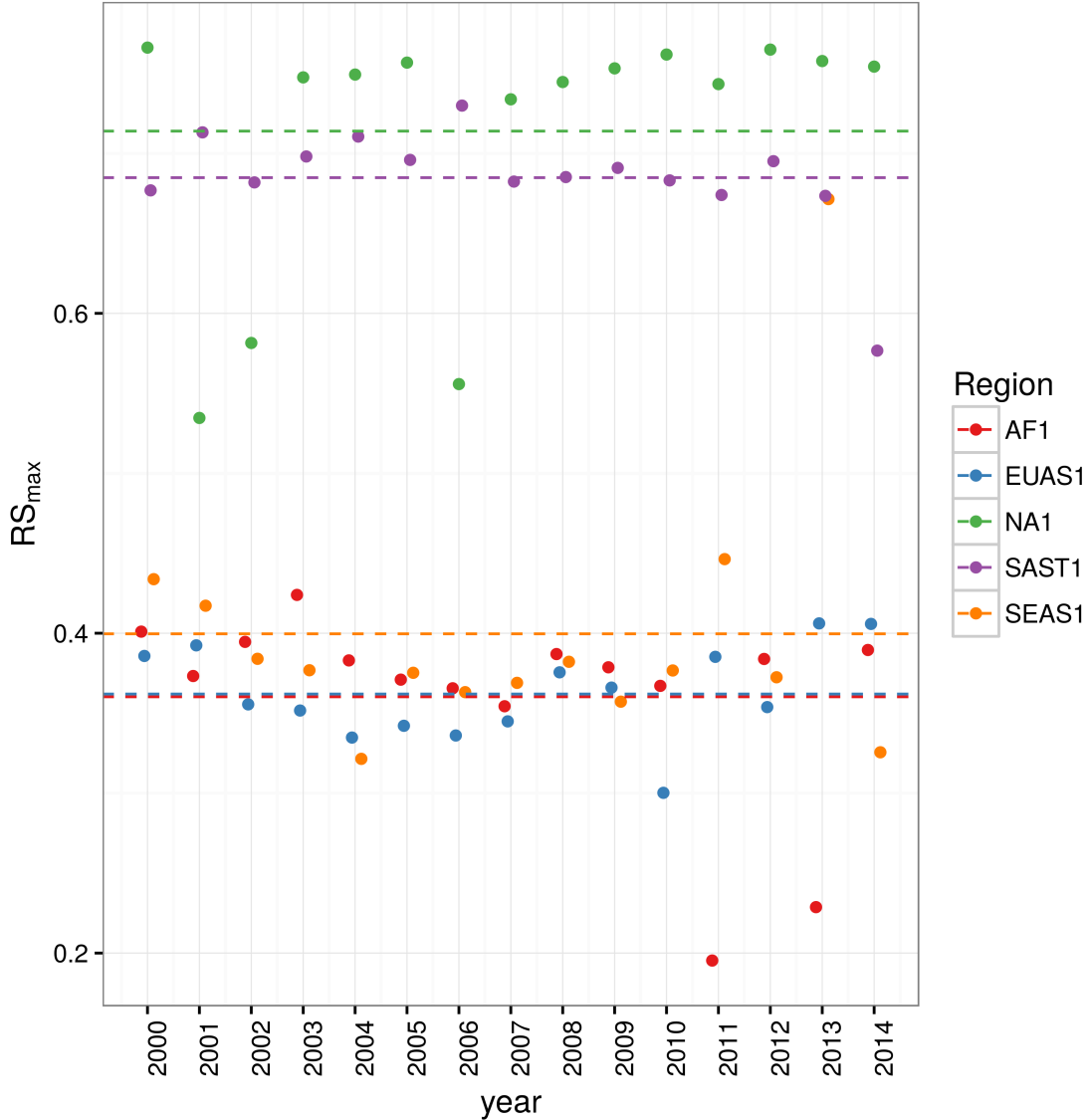


Figure 3: Largest patch proportion relative to total forest area RS_{max} , for regions with total forest area $> 10^7 \text{ km}^2$. Dashed lines are averages across time. The regions are AF1: Africa mainland, EUAS1: Eurasia mainland, NA1: North America mainland, SAST1: South America tropical and subtropical, SEAS1: Southeast Asia mainland.

278 and Java (OC7), all others were power laws (Appendix S4, Table S7). The goodness of fit test (GOF) did
279 not reject power laws in any case, but neither did it reject the other models except in a few cases; this was
280 due to the small number of observations. We only considered fluctuations to follow a power law when this
281 distribution was selected for both absolute and relative fluctuations.

282 The animations of the two largest patches (Appendix S3, largest patch gif animations) qualitatively shows
283 the nature of fluctuations and if the state of the forest is connected or not. If the largest patch is always
284 the same patch over time, the forest is probably not fragmented; this happens for regions with RS_{max} of
285 more than 40% such as AF2 (Madagascar), NA1 (North America), and OC3 (Malaysia). In the regions with
286 RS_{max} between 40% and 30% the identity of the largest patch could change or stay the same in time. For
287 OC7 (Java) the largest patch changes and for AF1 (Africa mainland) it stays the same. Only for EUAS1
288 (Eurasia mainland) we observed that the two largest patches are always the same, implying that this region
289 is probably composed of two independent domains and should be divided in further studies. The regions
290 with RS_{max} less than 25%: SAST2 (Cuba) and EUAS3 (United Kingdom), the largest patch always changes
291 reflecting their fragmented state. In the case of SEAS2 (Philippines) a transition is observed, with the
292 identity of the largest patch first variable, and then constant after 2010.

293 The results of quantile regressions are identical for ΔRS_{max} and ΔS_{max} (Appendix S4, table S4). Among the
294 biggest regions, Africa (AF1) has upper and lower quantiles with significantly negative slopes, but the lower
295 quantile slope is lower, implying that negative fluctuations and variance are increasing (Figure 4). Eurasia
296 mainland (EUAS1) has only the upper quantile significant with a positive slope, suggesting an increase in the
297 variance. North America mainland (NA1) exhibits a significant lower quantile with positive slope, implying
298 decreasing variance. Finally, for mainland Australia, all quantiles are significant, and the slope of the lower
299 quantiles is greater than the upper ones, showing that variance is decreasing (Appendix S4, figure S10).
300 These results are summarized in Table 1.

301 The conditions that indicate that a region is near a critical fragmentation threshold are that patch size
302 distributions follow a power law; temporal ΔRS_{max} fluctuations follow a power law; variance of ΔRS_{max} is
303 increasing in time; and skewness is negative. All these conditions were true only for Africa mainland (AF1)
304 and South America tropical & subtropical (SAST1).

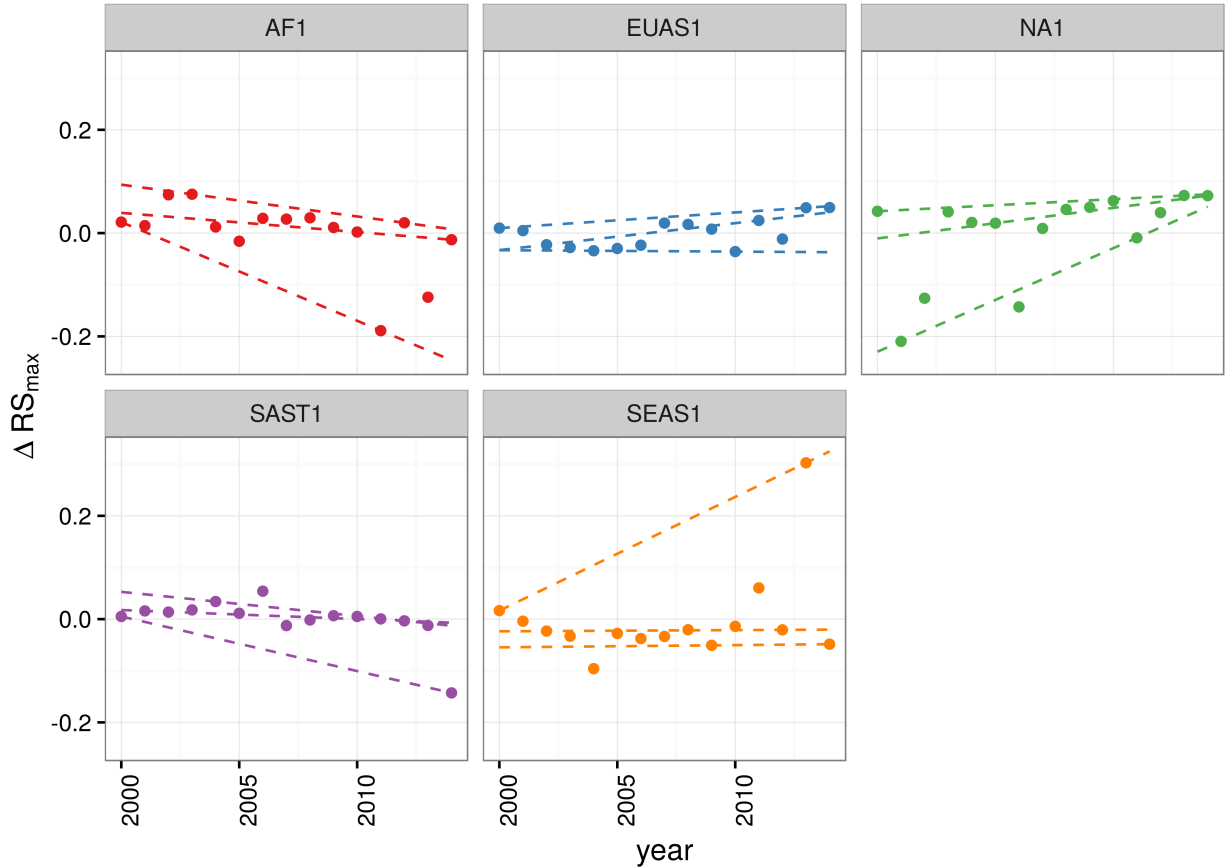


Figure 4: Largest patch fluctuations for regions with total forest area $> 10^7 \text{ km}^2$ across years. The patch sizes are relative to the total forest area of the same year. Dashed lines are 90%, 50% and 10% quantile regressions, to show if fluctuations were increasing. The regions are AF1: Africa mainland, EUAS1: Eurasia mainland, NA1: North America mainland, SAST1: South America tropical and subtropical, SEAS1: Southeast Asia mainland.

Table 1: Regions and indicators of closeness to a critical fragmentation threshold. Where, RS_{max} is the largest patch divided by the total forest area, ΔRS_{max} are the fluctuations of RS_{max} around the mean, skewness was calculated for RS_{max} and the increase or decrease in the variance was estimated using quantile regressions, NS means the results were non-significant.

Region		Description	Average	Patch Size	ΔRS_{max}	Skewness
			RS_{max}	Distrib	Distrib.	
AF	1	Africa mainland	0.36	Power	Power	-1.8630
	2	Madagascar	0.65	Power	Power	-0.2478
EUAS	1	Eurasia, mainland	0.36	LogNormal	Exp	0.4016
	2	Japan	0.94	Power	Power	0.0255
NA	1	United Kingdom	0.07	Power	Power	2.1330
	5	North America, mainland	0.71	Power	Power	-1.5690
OC	1	Newfoundland	0.87	Power	Power	-0.7411
	2	Australia, Mainland	0.28	Power	Power	0.0685
SAST	2	New Guinea	0.97	Power	Exp	0.1321
	3	Malaysia/Kalimantan	0.97	Power	Exp	-0.9633
SAT	4	Sumatra	0.92	Power	Power	1.3150
	5	Sulawesi	0.87	Power	Power	-0.3863
SEAS	6	New Zealand	0.76	Power	Exp	-0.6683
	7	South Island				
SAT	7	Java	0.38	Power	Exp	-0.1948
	8	New Zealand	0.75	Power	Exp	0.2940
SAST	8	North Island				
	1	South America, Tropical and subtropical forest up to Mexico	0.68	Power	Power	-2.7760
SAT	2	Cuba	0.21	Power	Power	0.2751
	1	South America, Temperate forest	0.60	Power	Power	-1.5070
SEAS	1	Southeast Asia, Mainland	0.40	Power	Power	3.0030

Region	Description	RS_{max}	Average	Patch Size	ΔRS_{max}
2	Philippines	0.54	Power	Power	Skewness

305 Discussion

306 We found that the forest patch distribution of most regions of the world followed power laws spanning
 307 seven orders of magnitude. These include tropical rainforest, boreal and temperate forest. Power laws have
 308 previously been found for several kinds of vegetation, but never at global scales as in this study. Interestingly,
 309 Eurasia does not follow a power law, but it is a geographically extended region, consisting of different domains
 310 (as we observed in the largest patch animations, Appendix S2). It is known that the union of two independent
 311 power law distributions produces a lognormal distribution (Rooij *et al.* 2013). Future studies should split
 312 this region into two or more new regions, and test if the underlying distributions are power laws.

313 Several mechanisms have been proposed for the emergence of power laws in forest: the first is related self
 314 organized criticality (SOC), when the system is driven by its internal dynamics to a critical state; this has
 315 been suggested mainly for fire-driven forests (Zinck & Grimm 2009; Hantson, Pueyo & Chuvieco 2015).
 316 Real ecosystems do not seem to meet the requirements of SOC dynamics: their dynamics are influenced by
 317 external forces, and interactions are non-homogeneous (i.e. vary from place to place) (Sole, Alonso & Mckane
 318 2002). Moreover, SOC requires a memory effect: fire scars in a site should accumulate and interfere with
 319 the propagation of a new fire. Pueyo *et al.* (2010) did not find such effect for tropical forests, and suggest
 320 that other mechanisms might produce the observed power laws. Other studies have also found that SOC
 321 models do not reproduce the patterns of observed fires (McKenzie & Kennedy 2012). Thus a mechanism
 322 which resembles SOC, i.e. with a double separation of scales, does not seem a plausible explanation for the
 323 global forest dynamics.

324 The mechanism suggested by Pueyo *et al.* (2010) is isotropic percolation, when a system is near the critical
 325 point power law structures arise. This is equivalent to the random forest model that we explained previously,
 326 and requires the tuning of an external environmental condition to carry the system to this point. We did not
 327 expect forest growth to be a random process at local scales, but it is possible that combinations of factors
 328 cancel out to produce seemingly random forest dynamics at large scales. If this is the case the power law
 329 exponent should be theoretically near $\alpha = 2.055$, but this value is outside the confidence interval we observed,
 330 and thus other explanations are needed.

331 The third mechanism suggested as the cause of pervasive power laws in patch size distribution is facilitation
332 (Manor & Shnerb 2008; Irvine, Bull & Keeling 2016): a patch surrounded by forest will have a smaller
333 probability of been deforested or degraded than an isolated patch. We hypothesize that models that include
334 facilitation could explain the patterns observed here. The model of Scanlon et al. (2007) represented the
335 dynamics of savanna trees includes a global constraint (mean rainfall), a local facilitation mechanism, and
336 two states (tree/non-tree), producing power laws across a rainfall gradient without the need for tuning an
337 external parameter. The results for this model showed an $\alpha = 1.34$ which is also different from our results.
338 Another model but with three states (tree/non-tree/degraded), including local facilitation and grazing, was
339 also used to obtain power laws patch distributions without external tuning, and exhibited deviations from
340 power laws at high grazing pressures (Kéfi *et al.* 2007). The values of the power law exponent α obtained
341 for this model are dependent on the intensity of facilitation, when facilitation is more intense the exponent
342 is higher, but the maximal values they obtained are still lower than the ones we observed. The interesting
343 point is that the value of the exponent is dependent on the parameters, and thus the observed α might
344 be obtained with some parameter combination. Kéfi *et al.* (2007) proposed that a deviation in power law
345 behavior with the form of an exponential decay or cut-off could be a signal of a critical transition. At the
346 continental scales studied here, we did not observe exponential cut-offs, but did observe other signals of a
347 transition. This confirms previous results (Weerman *et al.* 2012; Kéfi *et al.* 2014) showing that different
348 mechanisms can produce seemingly different spatial patterns near the transition, and that early warnings
349 based only on spatial patterns are not universal for all systems.

350 It has been suggested that a combination of spatial and temporal indicators could more reliably detect
351 critical transitions (Kéfi *et al.* 2014). In this study, we combined five criteria to detect the closeness to a
352 fragmentation threshold. Two of them were spatial: the forest patch size distribution, and the proportion
353 of the largest patch relative to total forest area (RS_{max}). The other three were the distribution of temporal
354 fluctuations in the largest patch size, the trend in the variance, and the skewness of the fluctuations. Each
355 one of these is not a strong individual predictor, but their combination gives us an increased degree of
356 confidence about the system being close to a critical transition.

357 We found that only the tropical forest of Africa and South America met all five criteria, and thus seem to
358 be near a critical fragmentation threshold. This means that the combined influence of human pressures and
359 climate forcings might trigger all the undesired effects of fragmentation in these extended areas. A small
360 but continuous increase in forest loss could produce a biodiversity collapse (Solé *et al.* 2004). This threshold
361 effect has been observed in different kind of models, experimental microcosms (Starzomski & Srivastava
362 2007), field studies (Pardini *et al.* 2010; Martensen *et al.* 2012) and food webs (Martinson, Fagan & Denno

363 Of these two areas, Africa seems to be more affected, because the proportion of the largest patch
364 relative to total forest area (RS_{max}) is near 30%, which could indicate that the transition is already started.
365 Moreover, this region was estimated to be potentially bistable, with the possibility to completely transform
366 into a savanna (Staver, Archibald & Levin 2011). The region of South America tropical forest has a RS_{max}
367 of more than 60% suggesting that the fragmentation transition is approaching but not yet started. The
368 island of Philippines (SEAS2) seems to be an example of a critical transition from an unconnected to a
369 connected state, the early warning signals can be qualitatively observed: a big fluctuation in a negative
370 direction precedes the transition and then RS_{max} stabilizes over 60%. This confirms that the early warning
371 indicators proposed here work in the correct direction.

372 At low levels of habitat reduction, species population will decline proportionally; this can happen even when
373 the habitat fragments retain connectivity. As habitat reduction continues, the critical threshold is approached
374 and connectivity will have large fluctuations (Brook *et al.* 2013). This could trigger several synergistic
375 effects: populations fluctuations and the possibility of extinctions will rise, increasing patch isolation and
376 decreasing connectivity (Brook *et al.* 2013). This positive feedback mechanism will be enhanced when the
377 fragmentation threshold is reached, resulting in the loss of most habitat specialist species at a landscape
378 scale (Pardini *et al.* 2010). Some authors argue that since species have heterogeneous responses to habitat
379 loss and fragmentation, and biotic dispersal is limited, the importance of thresholds is restricted to local
380 scales or even that its existence is questionable (Brook *et al.* 2013). Fragmentation is by definition a
381 local process that at some point produces emergent phenomena over the entire landscape, even if the area
382 considered is infinite (Oborny, Meszéna & Szabó 2005). In addition, after a region's fragmentation threshold
383 connectivity decreases, there is still a large and internally well connected patch that can maintain sensitive
384 species (Martensen *et al.* 2012). What is the time needed for these large patches to become fragmented, and
385 pose a real danger of extinction to a myriad of sensitive species? If a forest is already in a fragmented state, a
386 second critical transition from forest to non-forest could happen, this was called the desertification transition
387 (Corrado *et al.* 2014). Considering the actual trends of habitat loss, and studying the dynamics of non-forest
388 patches—instead of the forest patches as we did here—the risk of this kind of transition could be estimated.
389 To improve the estimation of non-forest patches other data set as the MODIS cropland probability should be
390 incorporated (Sexton *et al.* 2015). The simple models proposed previously could also be used to estimate if
391 these thresholds are likely to be continuous and reversible or discontinuous and irreversible, and the degree
392 of protection (e.g. using the set-asides strategy Banks-Leite *et al.* (2014)) than would be necessary to stop
393 this trend.

394 The effectiveness of landscape management is related to the degree of fragmentation, and the criteria to

395 direct reforestation efforts could be focused on regions near a transition (Oborny *et al.* 2007). Regions that
396 are in an unconnected state require large efforts to recover a connected state, but regions that are near a
397 transition could be easily pushed to a connected state; feedbacks due to facilitation mechanisms might help
398 to maintain this state. If the largest patch is always the same patch over time, the forest is probably not
399 fragmented. This patch could represent a core area for conservation, because it maintains the connectivity
400 of the whole region.

401 Crossing the fragmentation critical point in forests could have negative effects on biodiversity and ecosystem
402 services (Haddad *et al.* 2015), but it could also produce feedback loops at different levels of the biological
403 hierarchy. This means that a critical transition produced at a continental scale could have effects at the level
404 of communities, food webs, populations, phenotypes and genotypes (Barnosky *et al.* 2012). All these effects
405 interact with climate change, thus there is a potential production of cascading effects that could lead to a
406 global collapse. Therefore, even if critical thresholds are reached only in some forest regions at a continental
407 scale, a cascading effect with global consequences could still be produced, and may contribute to reach a
408 planetary tipping point (Reyer *et al.* 2015). The risk of such event will be higher if the dynamics of separate
409 continental regions are coupled (Lenton & Williams 2013). Using the time series obtained in this work the
410 coupling of the continental could be further investigated. It has been proposed that to assess the probability
411 of a global scale shift, different small scale ecosystems should be studied in parallel (Barnosky *et al.* 2012).
412 As forest comprises a major proportion of such ecosystems, we think that the transition of forests could be
413 used as a proxy for all the underling changes and as a successful predictor of a planetary tipping point.

414 Supporting information

415 **Appendix S1:** Supplementary data, Csv text file with model fits for patch size distribution, and model
416 selection for all the regions.

417 **Appendix S2:** Gif Animations of a forest model percolation. These are animations showing the subcritical,
418 critical, and super critical states.

419 **Appendix S3:** Gif Animations of largest patches. These show the temporal dynamics of the two largest
420 patches.

421 **Appendix S4:** Tables and figures.

422 *Table S1:* Proportion of Power law models not rejected by the goodness of fit test at $p \leq 0.05$ level.

423 *Table S2:* Generalized least squares fit by maximizing the restricted log-likelihood.

- ⁴²⁴ *Table S3:* Simultaneous Tests for General Linear Hypotheses of the power law exponent.
- ⁴²⁵ *Table S4:* Quantile regressions of the proportion of largest patch area vs year.
- ⁴²⁶ *Table S5:* Unbiased estimation of skewness for absolute largest patch fluctuations and relative fluctuations.
- ⁴²⁷ *Table S6:* Model selection using Akaike criterion for largest patch fluctuations in absolute values
- ⁴²⁸ *Table S7:* Model selection for fluctuation of largest patch in relative to total forest area.
- ⁴²⁹ *Figure S1:* Regions for Africa (AF), 1 Mainland, 2 Madagascar.
- ⁴³⁰ *Figure S2:* Regions for Eurasia (EUAS), 1 Mainland, 2 Japan, 3 United Kingdom.
- ⁴³¹ *Figure S3:* Regions for North America (NA), 1 Mainland, 5 Newfoundland.
- ⁴³² *Figure S4:* Regions for Australia and islands (OC), 1 Australia mainland; 2 New Guinea; 3 Malaysia/Kalimantan;
- ⁴³³ 4 Sumatra; 5 Sulawesi; 6 New Zealand south island; 7 Java; 8 New Zealand north island.
- ⁴³⁴ *Figure S5:* Regions for South America, SAST1 Tropical and subtropical forest up to Mexico; SAST2 Cuba;
- ⁴³⁵ SAT1 South America, Temperate forest.
- ⁴³⁶ *Figure S6:* Regions for Southeast Asia (SEAS), 1 Mainland; 2 Philippines.
- ⁴³⁷ *Figure S7:* Proportion of best models selected for patch size distributions using the Akaike criterion.
- ⁴³⁸ *Figure S8:* Power law exponents for forest patch distributions by year.
- ⁴³⁹ *Figure S9:* Largest patch proportion relative to total forest area RS_{max} , for regions with total forest area
- ⁴⁴⁰ less than 10^7 km^2 .
- ⁴⁴¹ *Figure S10:* Fluctuations of largest patch for regions with total forest area less than 10^7 km^2 . The patch
- ⁴⁴² sizes are relativized to the total forest area for that year.

⁴⁴³ Data Accessibility

- ⁴⁴⁴ The patch size files for all years and regions used here, and all the R and Matlab scripts are available at
- ⁴⁴⁵ figshare <http://dx.doi.org/10.6084/m9.figshare.4263905>.

⁴⁴⁶ BioSketch

- ⁴⁴⁷ Leonardo A. Saravia is a professor of the University of General Sarmiento (UNGS), Buenos Aires, Argentina.
- ⁴⁴⁸ He works with the Ecology group at the university with emphasis on community ecology and different kinds
- ⁴⁴⁹ of ecological networks focusing both on macroecological patterns and local processes. He is the leader of the

450 complex systems group of the UNGS institute of sciences, where the investigations are discussed with an
451 interdisciplinary point of view. The tools he uses are mainly computational, programming in C++ and R
452 statistical language.

453 **Acknowledgments**

454 LAS and SRD are grateful to the National University of General Sarmiento for financial support. This work
455 was partially supported by a grant from CONICET (PIO 144-20140100035-CO).

456 **References**

- 457 Allington, G.R.H. & Valone, T.J. (2010) Reversal of desertification: The role of physical and chemical soil
458 properties. *Journal of Arid Environments*, **74**, 973–977.
- 459 Banks-Leite, C., Pardini, R., Tambosi, L.R., Pearse, W.D., Bueno, A.A., Bruscagin, R.T., Condez, T.H.,
460 Dixo, M., Igari, A.T., Martensen, A.C. & Metzger, J.P. (2014) Using ecological thresholds to evaluate the
461 costs and benefits of set-asides in a biodiversity hotspot. *Science*, **345**, 1041–1045.
- 462 Barnosky, A.D., Hadly, E.A., Bascompte, J., Berlow, E.L., Brown, J.H., Fortelius, M., Getz, W.M., Harte, J.,
463 Hastings, A., Marquet, P.A., Martinez, N.D., Mooers, A., Roopnarine, P., Vermeij, G., Williams, J.W., Gille-
464 spie, R., Kitzes, J., Marshall, C., Matzke, N., Mindell, D.P., Revilla, E. & Smith, A.B. (2012) Approaching
465 a state shift in Earth’s biosphere. *Nature*, **486**, 52–58.
- 466 Bascompte, J. & Solé, R.V. (1996) Habitat fragmentation and extinction threholds in spatially explicit
467 models. *Journal of Animal Ecology*, **65**, 465–473.
- 468 Bazant, M.Z. (2000) Largest cluster in subcritical percolation. *Physical Review E*, **62**, 1660–1669.
- 469 Belward, A.S. (1996) *The IGBP-DIS Global 1 Km Land Cover Data Set “DISCover”: Proposal and Imple-
470 mentation Plans : Report of the Land Recover Working Group of IGBP-DIS*. IGBP-DIS Office.
- 471 Benedetti-Cecchi, L., Tamburello, L., Maggi, E. & Bulleri, F. (2015) Experimental Perturbations Modify the
472 Performance of Early Warning Indicators of Regime Shift. *Current biology*, **25**, 1867–1872.
- 473 Bestelmeyer, B.T., Ellison, A.M., Fraser, W.R., Gorman, K.B., Holbrook, S.J., Laney, C.M., Ohman, M.D.,
474 Peters, D.P.C., Pillsbury, F.C., Rassweiler, A., Schmitt, R.J. & Sharma, S. (2011) Analysis of abrupt tran-
475 sitions in ecological systems. *Ecosphere*, **2**, 129.
- 476 Boettiger, C. & Hastings, A. (2012) Quantifying limits to detection of early warning for critical transitions.

- 477 *Journal of The Royal Society Interface*, **9**, 2527–2539.
- 478 Bonan, G.B. (2008) Forests and Climate Change: forcings, Feedbacks, and the Climate Benefits of Forests.
- 479 *Science*, **320**, 1444–1449.
- 480 Botet, R. & Ploszajczak, M. (2004) Correlations in Finite Systems and Their Universal Scaling Properties.
- 481 *Nonequilibrium physics at short time scales: Formation of correlations* (ed K. Morawetz), pp. 445–466.
- 482 Springer-Verlag, Berlin Heidelberg.
- 483 Brook, B.W., Ellis, E.C., Perring, M.P., Mackay, A.W. & Blomqvist, L. (2013) Does the terrestrial biosphere have planetary tipping points? *Trends in Ecology & Evolution*.
- 484
- 485 Burnham, K. & Anderson, D.R. (2002) *Model selection and multi-model inference: A practical information-theoretic approach*, 2nd. ed. Springer-Verlag, New York.
- 486
- 487 Canfield, D.E., Glazer, A.N. & Falkowski, P.G. (2010) The Evolution and Future of Earth's Nitrogen Cycle.
- 488 *Science*, **330**, 192–196.
- 489 Carpenter, S.R., Cole, J.J., Pace, M.L., Batt, R., Brock, W.A., Cline, T., Coloso, J., Hodgson, J.R., Kitchell,
- 490 J.F., Seekell, D.A., Smith, L. & Weidel, B. (2011) Early Warnings of Regime Shifts: A Whole-Ecosystem
- 491 Experiment. *Science*, **332**, 1079–1082.
- 492 Clauset, A., Shalizi, C. & Newman, M. (2009) Power-Law Distributions in Empirical Data. *SIAM Review*,
- 493 **51**, 661–703.
- 494 Corrado, R., Cherubini, A.M. & Pennetta, C. (2014) Early warning signals of desertification transitions in
- 495 semiarid ecosystems. *Physical Review E - Statistical, Nonlinear, and Soft Matter Physics*, **90**, 62705.
- 496 Crowther, T.W., Glick, H.B., Covey, K.R., Bettigole, C., Maynard, D.S., Thomas, S.M., Smith, J.R., Hintler,
- 497 G., Duguid, M.C., Amatulli, G., Tuanmu, M.-N., Jetz, W., Salas, C., Stam, C., Piotto, D., Tavani, R., Green,
- 498 S., Bruce, G., Williams, S.J., Wiser, S.K., Huber, M.O., Hengeveld, G.M., Nabuurs, G.-J., Tikhonova, E.,
- 499 Borchardt, P., Li, C.-F., Powrie, L.W., Fischer, M., Hemp, A., Homeier, J., Cho, P., Vibrans, A.C., Umunay,
- 500 P.M., Piao, S.L., Rowe, C.W., Ashton, M.S., Crane, P.R. & Bradford, M.A. (2015) Mapping tree density at
- 501 a global scale. *Nature*, **525**, 201–205.
- 502 Dai, L., Vorselen, D., Korolev, K.S. & Gore, J. (2012) Generic Indicators for Loss of Resilience Before a
- 503 Tipping Point Leading to Population Collapse. *Science*, **336**, 1175–1177.
- 504 DiMiceli, C., Carroll, M., Sohlberg, R., Huang, C., Hansen, M. & Townshend, J. (2015) Annual Global
- 505 Automated MODIS Vegetation Continuous Fields (MOD44B) at 250 m Spatial Resolution for Data Years
- 506 Beginning Day 65, 2000 - 2014, Collection 051 Percent Tree Cover, University of Maryland, College Park,

- 507 MD, USA.
- 508 Drake, J.M. & Griffen, B.D. (2010) Early warning signals of extinction in deteriorating environments. *Nature*,
509 **467**, 456–459.
- 510 Efron, B. & Tibshirani, R.J. (1994) *An Introduction to the Bootstrap*. Taylor & Francis, New York.
- 511 Filotas, E., Parrott, L., Burton, P.J., Chazdon, R.L., Coates, K.D., Coll, L., Haeussler, S., Martin, K.,
512 Nocentini, S., Puettmann, K.J., Putz, F.E., Simard, S.W. & Messier, C. (2014) Viewing forests through the
513 lens of complex systems science. *Ecosphere*, **5**, 1–23.
- 514 Foley, J.A., Ramankutty, N., Brauman, K.A., Cassidy, E.S., Gerber, J.S., Johnston, M., Mueller, N.D.,
515 O’Connell, C., Ray, D.K., West, P.C., Balzer, C., Bennett, E.M., Carpenter, S.R., Hill, J., Monfreda, C.,
516 Polasky, S., Rockström, J., Sheehan, J., Siebert, S., Tilman, D. & Zaks, D.P.M. (2011) Solutions for a
517 cultivated planet. *Nature*, **478**, 337–342.
- 518 Folke, C., Jansson, Å., Rockström, J., Olsson, P., Carpenter, S.R., Iii, F.S.C., Crépin, A.-S., Daily, G.,
519 Danell, K., Ebbesson, J., Elmquist, T., Galaz, V., Moberg, F., Nilsson, M., Österblom, H., Ostrom, E.,
520 Persson, Å., Peterson, G., Polasky, S., Steffen, W., Walker, B. & Westley, F. (2011) Reconnecting to the
521 Biosphere. *AMBIO*, **40**, 719–738.
- 522 Fung, T., O’Dwyer, J.P., Rahman, K.A., Fletcher, C.D. & Chisholm, R.A. (2016) Reproducing static and
523 dynamic biodiversity patterns in tropical forests: the critical role of environmental variance. *Ecology*, **97**,
524 1207–1217.
- 525 Gardner, R.H. & Urban, D.L. (2007) Neutral models for testing landscape hypotheses. *Landscape Ecology*,
526 **22**, 15–29.
- 527 Gastner, M.T., Oborny, B., Zimmermann, D.K. & Pruessner, G. (2009) Transition from Connected to Frag-
528 mented Vegetation across an Environmental Gradient: Scaling Laws in Ecotone Geometry. *The American
529 Naturalist*, **174**, E23–E39.
- 530 Gillespie, C.S. (2015) Fitting Heavy Tailed Distributions: The poweRlaw Package. *Journal of Statistical
531 Software*, **64**, 1–16.
- 532 Gilman, S.E., Urban, M.C., Tewksbury, J., Gilchrist, G.W. & Holt, R.D. (2010) A framework for community
533 interactions under climate change. *Trends in Ecology & Evolution*, **25**, 325–331.
- 534 Goldstein, M.L., Morris, S.A. & Yen, G.G. (2004) Problems with fitting to the power-law distribution. *The
535 European Physical Journal B - Condensed Matter and Complex Systems*, **41**, 255–258.
- 536 Haddad, N.M., Brudvig, L.a., Clobert, J., Davies, K.F., Gonzalez, A., Holt, R.D., Lovejoy, T.E., Sexton,

- 537 J.O., Austin, M.P., Collins, C.D., Cook, W.M., Damschen, E.I., Ewers, R.M., Foster, B.L., Jenkins, C.N.,
538 King, a.J., Laurance, W.F., Levey, D.J., Margules, C.R., Melbourne, B.a., Nicholls, a.O., Orrock, J.L.,
539 Song, D.-X. & Townshend, J.R. (2015) Habitat fragmentation and its lasting impact on Earth's ecosystems.
540 *Science Advances*, **1**, 1–9.
- 541 Hantson, S., Pueyo, S. & Chuvieco, E. (2015) Global fire size distribution is driven by human impact and
542 climate. *Global Ecology and Biogeography*, **24**, 77–86.
- 543 Harris, T.E. (1974) Contact interactions on a lattice. *The Annals of Probability*, **2**, 969–988.
- 544 Hastings, A. & Wysham, D.B. (2010) Regime shifts in ecological systems can occur with no warning. *Ecology*
545 *Letters*, **13**, 464–472.
- 546 He, F. & Hubbell, S. (2003) Percolation Theory for the Distribution and Abundance of Species. *Physical*
547 *Review Letters*, **91**, 198103.
- 548 Hinrichsen, H. (2000) Non-equilibrium critical phenomena and phase transitions into absorbing states. *Ad-*
549 *vances in Physics*, **49**, 815–958.
- 550 Irvine, M.A., Bull, J.C. & Keeling, M.J. (2016) Aggregation dynamics explain vegetation patch-size distri-
551 butions. *Theoretical Population Biology*, **108**, 70–74.
- 552 Keitt, T.H., Urban, D.L. & Milne, B.T. (1997) Detecting critical scales in fragmented landscapes. *Conser-*
553 *vation Ecology*, **1**, 4.
- 554 Kéfi, S., Guttal, V., Brock, W.A., Carpenter, S.R., Ellison, A.M., Livina, V.N., Seekell, D.A., Scheffer, M.,
555 Nes, E.H. van & Dakos, V. (2014) Early Warning Signals of Ecological Transitions: Methods for Spatial
556 Patterns. *PLoS ONE*, **9**, e92097.
- 557 Kéfi, S., Rietkerk, M., Alados, C.L., Pueyo, Y., Papanastasis, V.P., ElAich, A. & Ruiter, P.C. de. (2007)
558 Spatial vegetation patterns and imminent desertification in Mediterranean arid ecosystems. *Nature*, **449**,
559 213–217.
- 560 Kitzberger, T., Aráoz, E., Gowda, J.H., Mermoz, M. & Morales, J.M. (2012) Decreases in Fire Spread Prob-
561 ability with Forest Age Promotes Alternative Community States, Reduced Resilience to Climate Variability
562 and Large Fire Regime Shifts. *Ecosystems*, **15**, 97–112.
- 563 Klaus, A., Yu, S. & Plenz, D. (2011) Statistical analyses support power law distributions found in neuronal

- 564 avalanches. (ed M Zochowski). *PloS one*, **6**, e19779.
- 565 Koenker, R. (2016) quantreg: Quantile Regression.
- 566 Leibold, M.A. & Norberg, J. (2004) Biodiversity in metacommunities: Plankton as complex adaptive sys-
567 tems? *Limnology and Oceanography*, **49**, 1278–1289.
- 568 Lenton, T.M. & Williams, H.T.P. (2013) On the origin of planetary-scale tipping points. *Trends in Ecology
569 & Evolution*, **28**, 380–382.
- 570 Loehle, C., Li, B.-L. & Sundell, R.C. (1996) Forest spread and phase transitions at forest-prairie ecotones in
571 Kansas, U.S.A. *Landscape Ecology*, **11**, 225–235.
- 572 Manor, A. & Shnerb, N.M. (2008) Origin of pareto-like spatial distributions in ecosystems. *Physical Review
573 Letters*, **101**, 268104.
- 574 Martensen, A.C., Ribeiro, M.C., Banks-Leite, C., Prado, P.I. & Metzger, J.P. (2012) Associations of Forest
575 Cover, Fragment Area, and Connectivity with Neotropical Understory Bird Species Richness and Abundance.
576 *Conservation Biology*, **26**, 1100–1111.
- 577 Martinson, H.M., Fagan, W.F. & Denno, R.F. (2012) Critical patch sizes for food-web modules. *Ecology*,
578 **93**, 1779–1786.
- 579 Martín, P.V., Bonachela, J.A., Levin, S.A. & Muñoz, M.A. (2015) Eluding catastrophic shifts. *Proceedings
580 of the National Academy of Sciences*, **112**, E1828–E1836.
- 581 McKenzie, D. & Kennedy, M.C. (2012) Power laws reveal phase transitions in landscape controls of fire
582 regimes. *Nat Commun*, **3**, 726.
- 583 Mitchell, M.G.E., Suarez-Castro, A.F., Martinez-Harms, M., Maron, M., McAlpine, C., Gaston, K.J., Jo-
584 hansen, K. & Rhodes, J.R. (2015) Reframing landscape fragmentation's effects on ecosystem services. *Trends
585 in Ecology & Evolution*, **30**, 190–198.
- 586 Naito, A.T. & Cairns, D.M. (2015) Patterns of shrub expansion in Alaskan arctic river corridors suggest
587 phase transition. *Ecology and Evolution*, **5**, 87–101.
- 588 Oborny, B., Meszéna, G. & Szabó, G. (2005) Dynamics of Populations on the Verge of Extinction. *Oikos*,
589 **109**, 291–296.
- 590 Oborny, B., Szabó, G. & Meszéna, G. (2007) Survival of species in patchy landscapes: percolation in space
591 and time. *Scaling biodiversity*, pp. 409–440. Cambridge University Press.
- 592 Ochoa-Quintero, J.M., Gardner, T.A., Rosa, I., de Barros Ferraz, S.F. & Sutherland, W.J. (2015) Thresholds

- 593 of species loss in Amazonian deforestation frontier landscapes. *Conservation Biology*, **29**, 440–451.
- 594 Ódor, G. (2004) Universality classes in nonequilibrium lattice systems. *Reviews of Modern Physics*, **76**,
595 663–724.
- 596 Pardini, R., Bueno, A. de A., Gardner, T.A., Prado, P.I. & Metzger, J.P. (2010) Beyond the Fragmentation
597 Threshold Hypothesis: Regime Shifts in Biodiversity Across Fragmented Landscapes. *PLoS ONE*, **5**, e13666.
- 598 Pinheiro, J., Bates, D., DebRoy, S., Sarkar, D. & R Core Team. (2016) *nlme: Linear and Nonlinear Mixed*
599 *Effects Models*.
- 600 Pueyo, S., de Alencastro Graça, P.M.L., Barbosa, R.I., Cots, R., Cardona, E. & Fearnside, P.M. (2010)
601 Testing for criticality in ecosystem dynamics: the case of Amazonian rainforest and savanna fire. *Ecology*
602 *Letters*, **13**, 793–802.
- 603 R Core Team. (2015) R: A Language and Environment for Statistical Computing.
- 604 Reyer, C.P.O., Rammig, A., Brouwers, N. & Langerwisch, F. (2015) Forest resilience, tipping points and
605 global change processes. *Journal of Ecology*, **103**, 1–4.
- 606 Rockstrom, J., Steffen, W., Noone, K., Persson, A., Chapin, F.S., Lambin, E.F., Lenton, T.M., Scheffer, M.,
607 Folke, C., Schellnhuber, H.J., Nykvist, B., Wit, C.A. de, Hughes, T., Leeuw, S. van der, Rodhe, H., Sorlin,
608 S., Snyder, P.K., Costanza, R., Svedin, U., Falkenmark, M., Karlberg, L., Corell, R.W., Fabry, V.J., Hansen,
609 J., Walker, B., Liverman, D., Richardson, K., Crutzen, P. & Foley, J.A. (2009) A safe operating space for
610 humanity. *Nature*, **461**, 472–475.
- 611 Rooij, M.M.J.W. van, Nash, B., Rajaraman, S. & Holden, J.G. (2013) A Fractal Approach to Dynamic
612 Inference and Distribution Analysis. *Frontiers in Physiology*, **4**.
- 613 Saravia, L.A. & Momo, F.R. (2017) Biodiversity collapse and early warning indicators in a spatial phase
614 transition between neutral and niche communities. *PeerJ PrePrints*, **5**, e1589v4.
- 615 Scanlon, T.M., Caylor, K.K., Levin, S.A. & Rodriguez-iturbe, I. (2007) Positive feedbacks promote power-law
616 clustering of Kalahari vegetation. *Nature*, **449**, 209–212.
- 617 Scheffer, M., Bascompte, J., Brock, W.A., Brovkin, V., Carpenter, S.R., Dakos, V., Held, H., Nes, E.H.V.,
618 Rietkerk, M. & Sugihara, G. (2009) Early-warning signals for critical transitions. *Nature*, **461**, 53–59.
- 619 Scheffer, M., Walker, B., Carpenter, S., Foley, J. a, Folke, C. & Walker, B. (2001) Catastrophic shifts in
620 ecosystems. *Nature*, **413**, 591–596.
- 621 Seidler, T.G. & Plotkin, J.B. (2006) Seed Dispersal and Spatial Pattern in Tropical Trees. *PLoS Biology*, **4**,

- 622 e344.
- 623 Sexton, J.O., Noojipady, P., Song, X.-P., Feng, M., Song, D.-X., Kim, D.-H., Anand, A., Huang, C., Channan,
624 S., Pimm, S.L. & Townshend, J.R. (2015) Conservation policy and the measurement of forests. *Nature
625 Climate Change*, **6**, 192–196.
- 626 Sole, R.V., Alonso, D. & Mckane, A. (2002) Self-organized instability in complex ecosystems. *Philosophical
627 transactions of the Royal Society of London. Series B, Biological sciences*, **357**, 667–681.
- 628 Solé, R.V. (2011) *Phase Transitions*. Princeton University Press.
- 629 Solé, R.V. & Bascompte, J. (2006) *Self-organization in complex ecosystems*. Princeton University Press, New
630 Jersey, USA.
- 631 Solé, R.V., Alonso, D. & Saldaña, J. (2004) Habitat fragmentation and biodiversity collapse in neutral
632 communities. *Ecological Complexity*, **1**, 65–75.
- 633 Solé, R.V., Bartumeus, F. & Gamarra, J.G.P. (2005) Gap percolation in rainforests. *Oikos*, **110**, 177–185.
- 634 Starzomski, B.M. & Srivastava, D.S. (2007) Landscape geometry determines community response to distur-
635 bance. *Oikos*, **116**, 690–699.
- 636 Stauffer, D. & Aharony, A. (1994) *Introduction To Percolation Theory*. Taylor & Francis, London.
- 637 Staver, A.C., Archibald, S. & Levin, S.A. (2011) The Global Extent and Determinants of Savanna and Forest
638 as Alternative Biome States. *Science*, **334**, 230–232.
- 639 Vasilakopoulos, P. & Marshall, C.T. (2015) Resilience and tipping points of an exploited fish population over
640 six decades. *Global Change Biology*, **21**, 1834–1847.
- 641 Weerman, E.J., Van Belzen, J., Rietkerk, M., Temmerman, S., Kéfi, S., Herman, P.M.J. & Koppell, J.V.
642 de. (2012) Changes in diatom patch-size distribution and degradation in a spatially self-organized intertidal
643 mudflat ecosystem. *Ecology*, **93**, 608–618.
- 644 Zhang, J.Y., Wang, Y., Zhao, X., Xie, G. & Zhang, T. (2005) Grassland recovery by protection from grazing
645 in a semi-arid sandy region of northern China. *New Zealand Journal of Agricultural Research*, **48**, 277–284.
- 646 Zinck, R.D. & Grimm, V. (2009) Unifying wildfire models from ecology and statistical physics. *The American
647 naturalist*, **174**, E170–85.
- 648 Zuur, A.F., Ieno, E.N., Walker, N., Saveliev, A.A. & Smith, G.M. (2009) *Mixed effects models and extensions
649 in ecology with R*. Springer New York, New York, NY.